Observation of few-cycle, strong-field phenomena in surface plasmon fields

P. Dombi,[1,*] S. E. Irvine,[2] P. Rácz,[1] M. Lenner,[1] N. Kroó,[1] G. Farkas,[1] A. Mitrofanov,[3] A. Baltuška,[3] T. Fuji,[4] F. Krausz,[4,5] and A. Y. Elezzabi[2]

[1]*Research Institute for Solid-State Physics and Optics, Konkoly-Thege M. út 29-33, 1121 Budapest, Hungary*
[2]*Ultrafast Optics and Nanophotonics Laboratory, University of Alberta, Edmonton, T6G 2V4, Canada*
[3]*Institut für Photonik, Technische Universität Wien, Gusshausstr. 27/387, 1040 Wien, Austria*
[4] *Max-Planck-Institut für Quantenoptik, Hans-Kopfermann-Strasse 1, 85748 Garching, Germany*
[5] *Ludwig-Maximilians-Universität, Am Coulombwall 1, 85748 Garching, Germany*
**dombi@szfki.hu*

Abstract: We present experimental evidence of the generation of few-cycle propagating surface plasmon polariton wavepackets. These ultrashort plasmonic pulses comprised of only 2-3 field oscillations were characterized by an autocorrelation measurement based on electron photoemission. By exploiting plasmonic field enhancement, we achieved plasmon-induced tunnelling emission from the metal surface at low laser intensity, opening perspectives for strong-field experiments with low pulse energies. All-optical electron acceleration up to keV kinetic energy is also demonstrated in these surface-confined, few-cycle fields with only 1.35×10^{12} W/cm^2 focused laser intensity. The experimental results are found to be in excellent agreement with the model.

OCIS codes: (240.6680) Surface plasmons; (320.7120) Ultrafast phenomena.

References and links

1. F. Krausz, and M. Yu. Ivanov, "Attosecond Physics," Rev. Mod. Phys. **81**, 163–234 (2009).
2. N. Engheta, A. Salandrino, and A. Alù, "Circuit elements at optical frequencies: nanoinductors, nanocapacitors, and nanoresistors," Phys. Rev. Lett. **95**(9), 095504 (2005).
3. S. I. Bozhevolnyi, V. S. Volkov, E. Devaux, J.-Y. Laluet, and T. W. Ebbesen, "Channel plasmon subwavelength waveguide components including interferometers and ring resonators," Nature **440**(7083), 508–511 (2006).
4. H. Ditlbacher, J. R. Krenn, G. Schider, A. Leitner, and F. R. Aussenegg, "Two-dimensional optics with surface plasmon polaritons," Appl. Phys. Lett. **81**, 1762–1764 (2002).
5. E. Cubukcu, E. A. Kort, K. B. Crozier, and F. Capasso, "Plasmonic laser antenna," Appl. Phys. Lett. **89**, 93120 (2006).
6. A. Kubo, K. Onda, H. Petek, Z. Sun, Y. S. Jung, and H. K. Kim, "Femtosecond imaging of surface plasmon dynamics in a nanostructured silver film," Nano Lett. **5**(6), 1123–1127 (2005).
7. T. Hanke, G. Krauss, D. Träutlein, B. Wild, R. Bratschitsch, and A. Leitenstorfer, "Efficient nonlinear light emission of single gold optical antennas driven by few-cycle near-infrared pulses," Phys. Rev. Lett. **103**(25), 257404 (2009).
8. S. Kim, J. H. Jin, Y. J. Kim, I. Y. Park, Y. Kim, and S. W. Kim, "High-harmonic generation by resonant plasmon field enhancement," Nature **453**(7196), 757–760 (2008).
9. J. Zawadzka, D. A. Jaroszynski, J. J. Carey, and K. Wynne, "Evanescent-wave acceleration of ultrashort electron pulses," Appl. Phys. Lett. **79**, 2130–2132 (2001).
10. J. Kupersztych, P. Monchicourt, and M. Raynaud, "Ponderomotive acceleration of photoelectrons in surface-plasmon-assisted multiphoton photoelectric emission," Phys. Rev. Lett. **86**(22), 5180–5183 (2001).
11. S. E. Irvine, A. Dechant, and A. Y. Elezzabi, "Generation of 0.4-keV femtosecond electron pulses using impulsively excited surface plasmons," Phys. Rev. Lett. **93**(18), 184801 (2004).
12. M. I. Stockman, M. F. Kling, U. Kleineberg, and F. Krausz, "Attosecond nanoplasmonic-field microscope," Nature Photon. **1**, 539–544 (2007).
13. C. Ropers, D. R. Solli, C. P. Schulz, C. Lienau, and T. Elsaesser, "Localized multiphoton emission of femtosecond electron pulses from metal nanotips," Phys. Rev. Lett. **98**(4), 043907 (2007).
14. P. Hommelhoff, C. Kealhofer, and M. A. Kasevich, "Ultrafast electron pulses from a tungsten tip triggered by low-power femtosecond laser pulses," Phys. Rev. Lett. **97**(24), 247402 (2006).
15. A. Bouhelier, and G. P. Wiederrecht, "Surface plasmon rainbow jets," Opt. Lett. **30**(8), 884–886 (2005).
16. A. W. Dweydari, and C. H. B. Mee, "Work function measurements on (100) and (110) surfaces of silver," Phys. Status Solidi **27**, 223 (1975) (a).

#135646 - $15.00 USD Received 24 Sep 2010; revised 22 Oct 2010; accepted 25 Oct 2010; published 3 Nov 2010

17. H. Petek, and S. Ogawa, "Femtosecond time-resolved two-photon photoemission studies of electron dynamics in metals," Prog. Surf. Sci. **4**, 239–310 (1997).
18. S. E. Irvine, and A. Y. Elezzabi, "Surface-plasmon-based electron acceleration," Phys. Rev. A **73**, 013815 (2006).
19. N. Kroo, J.-P. Thost, M. Völcker, W. Krieger, and H. Walther, "Decay length of surface-plasmons determined with a tunneling microscope," Europhys. Lett. **15**, 289 (1991).
20. Y. Leroux, J. C. Lacroix, C. Fave, V. Stockhausen, N. Félidj, J. Grand, A. Hohenau, and J. R. Krenn, "Active plasmonic devices with anisotropic optical response: a step toward active polarizer," Nano Lett. **9**(5), 2144–2148 (2009) (and references therein).
21. B. Lamprecht, J. R. Krenn, A. Leitner, and F. R. Aussenegg, "Particle-plasmon decay-time determination by measuring the optical near field's autocorrelation: influence of inhomogeneous line broadening," Appl. Phys. B **69**, 223–227 (1999).
22. L. V. Keldysh, "Ionization in the field of a strong electromagnetic wave," Sov. Phys. JETP **20**, 1307 (1965).
23. H. Raether, Surface plasmons on Smooth and Rough Surfaces and on Gratings, (Springer, Berlin, 1988).
24. G. Farkas, and C. Tóth, "Energy spectrum of photoelectrons produced by picosecond laser-induced surface multiphoton photoeffect," Phys. Rev. A **41**(7), 4123–4126 (1990).
25. P. Dombi, and P. Rácz, "Ultrafast monoenergetic electron source by optical waveform control of surface plasmons," Opt. Express **16**(5), 2887–2893 (2008).

1. Introduction

Recent progress in femtosecond laser technology enabled the generation of few-cycle optical waveforms, revolutionizing atomic physics by enabling, for the first time, controlled generation and measurement of isolated attosecond pulses [1]. In a parallel development, significant advances have been reported in the field of plasmonics including the fabrication and study of integrated plasmonic/nano-optical components [2–5], nonlinear processes taking place in localized fields [6–8] and fundamental physical studies of plasmonic electron emission phenomena [9–12], to name a few. In spite of these advances, the potential lying in the synergistic merger of few-cycle optics with plasmonics is yet to be exploited. This is especially true for the generation of propagating surface plasmon polaritons (SPPs) that are particularly suitable for the investigation of the strong-field aspect of plasmonics in simple configurations. The generation of few-cycle plasmonic waveforms can bring benefits for any application where photoemitted, all-optically accelerated as well as rescattering electrons play an important role in the physical process under study.

In order to demonstrate this potential experimentally, we set out to investigate how few-cycle laser pulses can be coupled to propagating ultrashort SPPs. We generated few-cycle SPP wavepackets and characterized their temporal properties. We also demonstrated that resonant SPP field enhancement, along with its sub-wavelength confinement at a metallic surface, can be exploited to investigate nonlinear field-driven processes at low laser pulse powers. While localized field enhancement at a dc-biased metal tip was utilized in multiphoton or photofield emission studies [13,14], strong-field effects of propagating SPPs have not been investigated. Therefore, as a direct application of few-cycle plasmonics, we demonstrate, for the first time, strong-field electron acceleration in the evanescent electric field of few-cycle SPP pulses.

2. Time-resolved experiments on few-cycle plasmonic photoemission

In order to generate few-cycle SPPs, we focused the output of an ultra-broadband laser oscillator delivering 5 fs laser pulses (with 5 nJ pulse energy having a central wavelength of 795 nm) onto a 50 nm thick silver film sputter-coated onto the face of a right-angle prism in the Kretschmann configuration (Fig. 1). Broadband SPP coupling is confirmed by the absence of reflected light. While it is known that this configuration, together with a collimated laser beam, restricts the bandwidth of light-SPP coupling, by employing a focused beam, such a constraint was eliminated. The resulting spread of *k*-vectors of the incident beam ensures that all spectral components are coupled to the SPP exciation. The typical focused spot size and intensity were ~9 μm and 3×10^8 W/cm^2, respectively. While broadband SPP coupling setups investigated in the spectral domain are known [15], we set out to characterize propagating SPPs temporally with an ultrahigh time resolution. To this end, electron emission from the surface was monitored without influencing SPP generation. As the plasmonic field generates

#135646 - $15.00 USD Received 24 Sep 2010; revised 22 Oct 2010; accepted 25 Oct 2010; published 3 Nov 2010

multi-photon-induced (nonlinear) electron emission at the metal-vacuum interface, the evolution of the SPP wavepacket was characterized via a higher order autocorrelation experiment with multi-photon photoemission playing the role of the nonlinear detector.

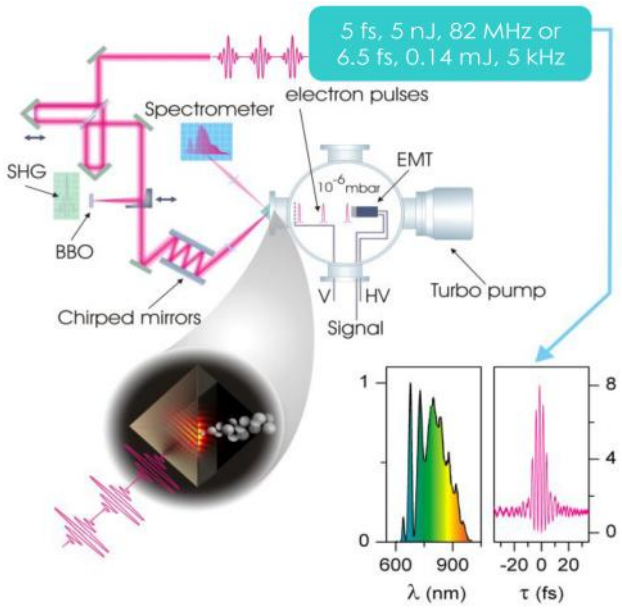

Fig. 1. Experimental scheme with pulse parameters and characterization results of a 5-fs, 5-nJ pulse (spectrum and second order autocorrelation are shown in the insets). SHG: second harmonic generation-based autocorrelation, BBO: β-BaB_2O_4 crystal, EMT: electron multiplier tube (Hamamatsu R595), HV: high voltage, V: retarding grid voltage feedthrough. Pulse propagation in the prism material was pre-compensated for by introducing broadband chirped mirrors and finely tuneable dispersive elements (a pair of thin glass wedges) into the beam.

First, we measured the nonlinearity by detecting photoemitted electrons on the vacuum side of the surface with the prism acting as vacuum window (Fig. 1.). In this intensity regime, we observed a fourth order SPP-induced electron emission process corresponding to the ~1.5 eV photon energy and ~4.62 eV work function of the silver thin film [16]. The measured photocurrent j as a function of the laser pulse intensity I_l shows excellent agreement with the fourth-order intensity dependence ($j \propto I_l^{n=4.05\pm0.11}$, see inset in Fig. 2(a)), thereby confirming the emission mechanism and the multi-photon ansatz for further evaluations. When the laser beam is detuned from its optimum SPP coupling angle, the SPP resonance disappears and no electrons are detected. This confirms that it is the SPP field that causes electron emission and thus the time-resolved measurement is sensitive to the temporal evolution of this field only.

To gain an insight into the temporal evolution of the SPP process, we applied the concept of time-resolved photoemission to the present experimental investigation [17]. Here, time-resolved SPP photoemission was measured via the use of a broadband interferometric autocorrelator (Fig. 1). We detected the plasmonic photocurrent, j, as a function of the delay, τ, between two incident laser pulse replicas. The result is depicted in Fig. 2(a). The measured signal clearly reproduces the fourth order autocorrelation function of a few-cycle pulse and promptly signifies the ultrashort, few-cycle nature of the SPP wavepacket.

In order to evaluate this result quantitatively, we simulated this measurement exactly for the experimentally generated SPP fields on the metal surface. We determined these SPP fields based on a first-principles approach, without employing any fitting parameters, by solving Maxwell's equations for the given SPP coupling geometry using a finite-difference time-domain method [18]. The modelled Ag film exhibited 2.8 nm rms roughness, corresponding exactly to the measured surface profile of the experimental sample.

#135646 - $15.00 USD Received 24 Sep 2010; revised 22 Oct 2010; accepted 25 Oct 2010; published 3 Nov 2010

The temporal distribution of the SPP electric field, $E_{SPP}(t,r)$, was evaluated at several locations on the metallic surface. Then, the resulting SPP pulses at each surface location, r_i, were delayed in time by τ and added interferometrically to establish the field evolution realized by the interferometric setup (Fig. 1); $\tilde{E}_{SPP}(t,r_i,\tau) = E_{SPP}(t,r_i) + E_{SPP}(t+\tau,r_i)$. If we denote the intensity envelope of this waveform with $\tilde{I}_{SPP}(t,r_i,\tau)$, the total photoemitted charge can be calculated for each grid point on the surface via $\tilde{j}(r_i,\tau) = \int_t \tilde{I}^4_{SPP}(t,r_i,\tau)dt$; where the fourth power of the intensity corresponds to the fourth order multiphoton process determining the emission profile (as evidenced by the inset of Fig. 2(a)). By integrating the photoemitted charge over the whole surface, we determine the total signal for a given delay between the two pulses, $j(\tau) = \sum_i \tilde{j}(r_i,\tau)$. The function $j(\tau)$ for the given input pulse and surface was computed and plotted in Fig. 2(b) (blue curve).

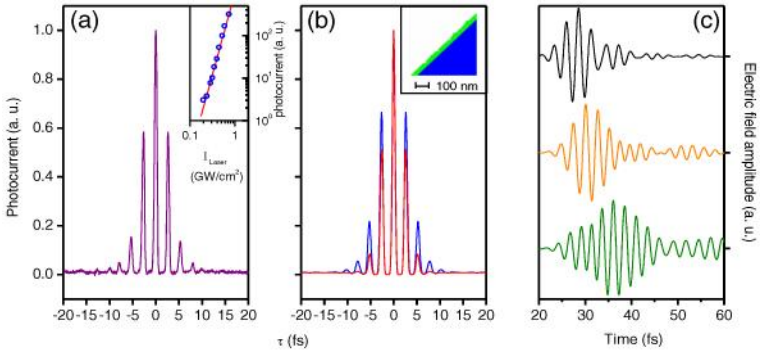

Fig. 2. (a) Measured interferometric time-resolved signal of SPP enhanced photoemission induced by few-cycle pulses. The reconstructed blue curve in (b) is calculated using the simulation of SPP coupling on the actual, sputtered metal film with 5-fs exciting laser pulses (see text for details and also the inset of (b) for the illustration of a part of the modelling geometry with the prism material in blue and the sputtered silver film in green). The red curve in (b) is the calculated fourth order autocorrelation function of the SPP exciting 5-fs laser pulse, plotted for reference. The inset of (a) illustrates the fourth order dependence of the total SPP-induced free-space photocurrent on a double logarithmic scale. The slope of the fit is n = 4.05 ± 0.11. The curves in (c) are typical computed few-cycle SPP waveforms at different locations on the Ag surface exhibiting 2.8 nm rms roughness.

There is good agreement with the measured curve in Fig. 2(a). The 15% mismatch between the measured and calculated time-resolved signal widths is attributed to mismatch between the exact surface profile of the Ag film and the simulated one. As a further reference, we also plotted the fourth order autocorrelation function of the incident laser pulse (Fig. 2(b), red curve). This is 12% shorter than the measured curve, in accordance with expectations to be discussed below. These results clearly show that photoemission by the propagating SPP wave causes the measured fringe-resolved signal in our experiments. The reconstruction procedure models exactly all relevant elements of SPP coupling, plasmonic photoemission, and consistently yields the time-resolved photoemission trace for the given surface.

Additionally, we examined the temporal evolution of these plasmonic fields $E_{SPP}(t,r_i)$, that are directly extracted from these simulations for some representative locations on the illuminated surface. Figure 2(c) depicts some typical SPP wavepackets having durations ranging from 5.6 fs to 9 fs over the spot examined. These few-cycle propagating SPP pulses are slightly longer than the exciting laser pulse due to a slight bandwidth loss upon SPP coupling. After few-cycle SPP excitation over a focal spot of ~9 μm diameter, the SPP propagates only some 34 μm further down on the surface until it decays due to substantial propagation losses [19]. However, due to the $j \propto I_l^{n\,=\,4.05\,\pm\,0.11}$ dependence, the spatial profile of the photocurrent distribution (the $j(r)$ curve) decays within ~8.5 μm in the direction of the SPP propagation. This is comparable to the illuminated focal spot size which means that the time-

#135646 - $15.00 USD Received 24 Sep 2010; revised 22 Oct 2010; accepted 25 Oct 2010; published 3 Nov 2010

resolved photoemission autocorrelation signal is built up of mainly those electrons that are emitted from the central part of the illuminated spot where the plasmonic pulse does not yet significantly broaden due to dispersion. Thus, this analysis confirms few-cycle SPP generation, opening the doorway to applications in broadband, few-cycle plasmonics.

Our experimental results supported by simulation also readily suggest that no localized and decoupled plasmon modes are excited, but rather propagating ultrashort SPP wavepackets strongly coupled to the film surface dominate the interaction process. If the photoemission process was due to localized plasmons, the corresponding temporal evolution of the electric field would have been significantly longer on at least some surface locations due to the narrow SPP resonance, a known phenomenon for nanoparticles and nanostructures [20]. This implies that inhomogeneous broadening effects typical for localized plasmon excitation on physically isolated metal nanoparticles having distinct particle plasmon resonances do not contribute to the temporal shape of the measured time-resolved signal [21]. Thus, the curve in Fig. 2(a) represents a true characterization of the SPP wavepacket launched by few-cycle pulses.

3. Spectrally resolved measurements of few-cycle plasmonic electron acceleration

By spectroscopic characterization of ultrafast electron bunches resulting from plasmonic emission processes, we can reveal further intriguing phenomena taking place in few-cycle SPP fields. To this end, we performed measurements at much higher intensities with a different few-cycle laser system based on a multipass Ti:sapphire amplifier delivering 800-nm, 6.5-fs pulses with 5 kHz. The maximum pulse energy used for the experiments was 140 μJ. The setup contained a retarding potential analyzer for electron kinetic energy measurements. Figure 3(a) shows measured energy distributions at different laser intensities (measured at the surface without accounting for SPP field enhancement) where the highest focused intensity of 1.35×10^{12} W/cm^2 is just below the damage threshold intensity of the Ag film (~1.5×10^{12} W/cm^2, as we observed). Remarkably, energy levels approaching 1 keV can be reached within the short-lived evanescent SPP field (Fig. 3(b), red circles).

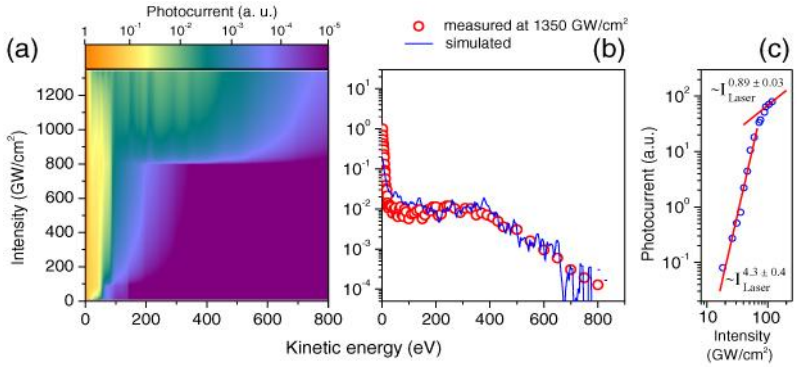

Fig. 3. (a) Few-cycle SPP accelerated electron spectra at different intensities. The spectrum corresponding to the highest 1.35×10^{12} W/cm^2 focused intensity is depicted in (b) (red circles) together with the corresponding simulation result (blue solid line, see text). (c) shows the total electron yield as a function of intensity on a log-log scale. The decrease of the slope from a value of 4.3 to 0.89 corresponds to the transition between multi-photon and tunneling emission.

Due to the fact that the field extends to only a fraction of a wavelength away from the silver surface (~250 nm) and that the temporal duration of the plasmonic wavepacket is only a few optical cycles, keV acceleration takes place within the ultrashort residence time of the electron in the SPP field, confirming the robustness of this all-optical electron generation and acceleration setup. At the highest laser intensity of 1.35×10^{12} W/cm^2, we estimate the number of electrons collected by the electron multiplier tube to be around 1.5×10^4 electrons/pulse from typical multiplier gain. Even if we generate significantly more electrons than those collected, we still conclude that space charge effects do not distort the spectra according to

#135646 - $15.00 USD Received 24 Sep 2010; revised 22 Oct 2010; accepted 25 Oct 2010; published 3 Nov 2010

simulations with the General Particle Tracer (GPT) code. We found that space-charge-based distortions set in at around 10^7-10^8 electrons/pulse with the actual experimental setup.

By analyzing the results further, we found that at the highest intensity used (1.35×10^{12} W/cm^2) the multi-photon ansatz for the plasmonic photoemission is not valid any more, but strong-field phenomena dominate the process. First, we determined the Keldysh parameter γ for each intensity used during the experiments. γ is a well-known metric used to classify photoemission or atomic photo-ionization processes [22]. The intensity at which multi-photon-induced photoemission turns into tunnelling occurs when $\gamma \cong 1$ both for atoms and surfaces (i.e., when the peak laser field is comparable to the electron binding field).

As shown in Fig. 3(c), this behaviour is manifested as a transition in the SPP-emitted photocurrent curve as a function of the laser intensity. The transition from the fourth order power law dependence ($j \propto I_l^{\,n = 4.3 \pm 0.4}$) to a $j \propto I_l^{\,n = 0.89 \pm 0.03}$ dependence is evident in Fig. 3(c). If we carried out a simple photoemission experiment at a bulk metal surface without SPP excitation, this indicative transition at $\gamma \cong 1$ would have happened at around 3.6×10^{13} W/cm^2 focused intensity. Since this change appears at much lower laser intensities ($\gamma >> 1$), we conclude again that the field inducing the photoemission is not that of the laser pulse, but that of the SPP. By analyzing the I_l-j curve and γ, we estimate the *average effective* field enhancement factor to be 21.4±2.3; and thus strong-field transitions can be reached at very low focused intensities of around 10^{11} W/cm^2. We have to note that a perfectly smooth silver surface yields an enhancement value of 14.6 [23]. The fact that the average effective enhancement is somewhat higher is a result of the slight, 2.8 nm rms roughness of the actual surface. Field enhancement values around 15-25 raise the kinetic energy of the accelerated electrons by several hundred times, proportionally to the intensity, according to ponderomotive scaling.

Of great interest is the particular energy distribution of the emitted electrons, too. Therefore, we simulated the SPP field distribution at the surface, as described above. The field values are then used to calculate a weight factor for each surface emitted test electron that is placed in an equidistant fashion, spatially and temporally, around the SPP wave. The weight factor is determined according to a Fowler-Nordheim-type tunnelling profile, yielding emission probabilities as a function of instantaneous field strength at each location [14]. The free electron motion is then calculated with the Lorentz force equation in the SPP field. Next, test electrons are binned according to their final energy to form the kinetic energy spectra. The electron spectrum resulting from this simulation for 1.35×10^{12} W/cm^2 incident intensity is depicted in Fig. 3(b), corresponding remarkably well to the measured electron spectrum. This semi-classical simulation accounts for the characteristic shape of measured spectra.

In addition, there are some more sophisticated features in the measured spectra, such as the appearance of a broader plateau at 8×10^{11} W/cm^2 focused laser intensity and the oscillatory spectral structures superimposed on this plateau above 10^{12} W/cm^2. Both of them could be attributed to above threshold photoemission (ATP) electrons [24], obviously not accounted for in our simulations based on a semi-classical model. The confirmation of the contribution of this phenomenon necessitates further, more sophisticated theoretical studies. Note, however, that the overall number of electrons steadily increases toward higher intensities and the relative weight of any potential ATP electrons in the spectrum does not change significantly. Therefore, it is clear that mainly Lorentz-force acceleration determines the spectral shape even at the highest intensities, as also evidenced by our simulation results in Fig. 3(b).

4. Summary and conclusions

We demonstrated the generation of few-cycle SPP waveforms excited by an ultrashort laser pulse. Strong-field SPPs were exploited to generate high-energy electrons efficiently in an all-optical manner. We have shown that tunnel emission processes play a key role in these interactions thanks to SPP field enhancement. By exploiting this, strong-field interactions can be accessed at much lower laser intensities, revealing a new paradigm for the interaction of high optical fields with matter employing low-energy pulses. From a practical standpoint, our

#135646 - $15.00 USD Received 24 Sep 2010; revised 22 Oct 2010; accepted 25 Oct 2010; published 3 Nov 2010

setup integrates a photocathode and all-optical electron acceleration into an ultra-compact scheme. As an application, we envisage highly synchronized, all-optically generated electron sources from nano-patterned surfaces for time-resolved measurements [25]. This feature is also attractive for novel ultrafast/plasmonic pump-probe schemes. The combination of few-cycle, high-intensity fields with plasmonics promises to expand our knowledge of ultrafast, strong-field nanoscale events.

Acknowledgements

We wish to acknowledge Kárpát Ferencz and György Molnár for sample preparation and László Veisz for modelling electron bunch propagation and potential space charge effects. The Hungarian Scientific Research Fund (Projects 73728, 81364) and the Natural Sciences and Engineering Research Council of Canada provided financial support.

#135646 - $15.00 USD Received 24 Sep 2010; revised 22 Oct 2010; accepted 25 Oct 2010; published 3 Nov 2010